International Journal of Mechanical and Electrical Engineering
ISSN: 3005-9615 (Print), ISSN: 3005-7132 (Online) | Volume 7, Number 2, Year 2025
DOI: https://doi.org/10.62051/ijmee.v7n2.03
Journal homepage: https://wepub.org/index.php/IJMEE/index

Dimensionless Analysis of Centrifugal Fan Characteristics: Experimental Evaluation at Three Rotational Speeds

Xinrui Xu

Faculty of Science and Engineering, The University of Nottingham Ningbo China, Ningbo, Zhejiang, 315199, China

ABSTRACT

The aerodynamic performance of centrifugal fans has been studied due to their wide application in industrial and engineering fields such as ventilation, air circulation, and thermal management. This paper investigates the performance characteristics of a backward-curved blade centrifugal fan at approximately 1000, 2000, and 2700 rpm through experimental methods. The experimental apparatus comprised a calibrated nozzle, diffuser, universal dynamometer, slide valve, and digital pressure display for precise measurement of pressure rise, volumetric flow rate, electrical power, and efficiency. By progressively altering the slide valve opening, pressure-difference versus flow rate curves and efficiency versus flow rate curves were obtained. The results demonstrated typical centrifugal fan characteristics: pressure rise initially increased then decreased with rising volumetric flow rate, while efficiency peaked at medium-to-high flow rates. To validate hydrodynamic similarity, dimensionless parameters including flow coefficient, pressure difference coefficient, and power coefficient were calculated. Results demonstrate that the dimensionless pressure and power curves at different rotational speeds largely coincide, confirming the principle of dynamic similarity. However, significant deviations occur at low rotational speeds, primarily attributed to increased friction losses, flow separation, and slip effects. This study confirms the applicability of dynamic similarity in centrifugal fans and reveals the influence of Reynolds number and efficiency variations under low-speed conditions, providing a reference for fan design optimization and performance prediction.

KEYWORDS

Centrifugal Fan; Performance Characteristics; Dynamic Similarity; Nondimensional Analysis; Efficiency; Experimental Investigation.

1. INTRODUCTION

1.1. Brief Background

This experiment focuses on analyzing the characteristics of a centrifugal fan with backward facing blades at different rotational speeds. A centrifugal fan exerts energy on the air through the rotation of the impeller, pushing the air in a direction perpendicular to its axis. By measuring the inlet nozzle, before and after the fans pressure, flow rates and power consumptions, the dynamic similarity of the fan at different speeds can be investigated.

Centrifugal fans are commonly used in ventilation and cooling systems because they can generate higher pressure rises than axial fans at relatively low flow rates. Their performance is usually described by characteristic curves that relate pressure, flow rate, and efficiency.

Content from this work may be used under the terms of CC BY-NC 4.0 licence (https://creativecommons.org/licenses/by-nc/4.0/).
Published by Warwick Evans Publishing.

The principle of dynamic similarity is important for turbomachinery. When fans are geometrically similar and operate under the same nondimensional parameters, their performance trends can be compared directly. Verifying this principle in experiments provides useful insight for predicting and scaling fan behavior.

1.2. Objectives

The objectives of the experiment were to determine the characteristics of a centrifugal fan at three different rotational speeds. Investigating the effectiveness of dynamic similarity of the fan characteristics at three different fan speeds.

2. METHODOLOGY

2.1. Apparatus

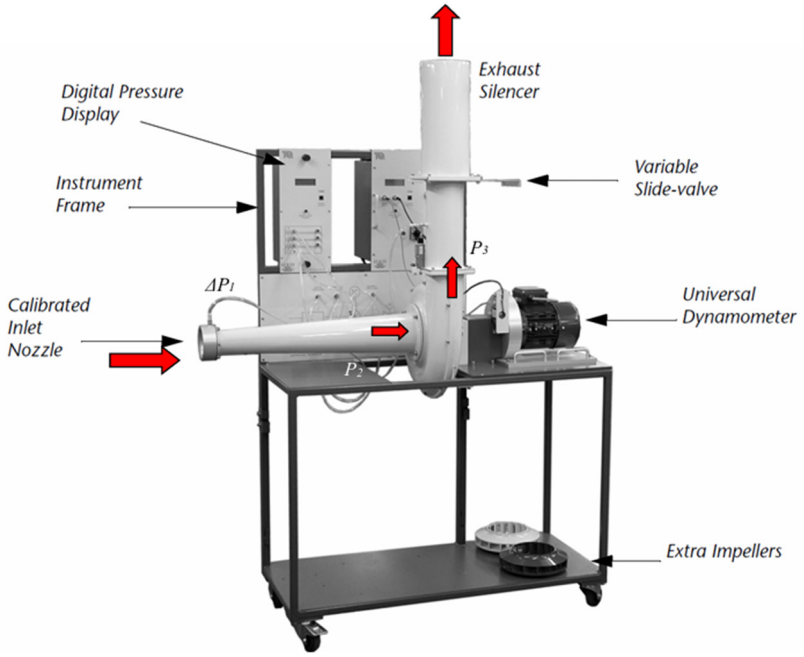

Figure 1. Apparatus used for the laboratory

Figure 1 illustrates the main apparatus used during the Centrifugal Fan Module, which is as follows:

(a) Calibrated inlet nozzle: Calibration nozzle installed at the inlet of the fan. The calibrated inlet nozzle is the entrance for air into the casing, ensures uniform airflow into the system, reducing turbulence.

(b) Diffuser: The diffuser is behind the nozzle. It is used to stabilize the air flow, reduce turbulence at the fan inlet and ensure that the air enters the fan blade smoothly.

(c) Fan: Centrifugal fans with backward inclined blades allow air to enter axially and exit radially. By adjusting the rotational speed of the fan, it is possible to investigate the variability of the fan characteristics at different rotational speeds.

(d) Universal dynamometer: The Universal dynamometer links to the rotor of the fan, and controls the speed of the fan, adjusting it from 1000 to 3000 rpm.

(e) Variable slide valve: Slide valve used to adjust the air flow to the fan, which can be adjusted from 0 % to 100 %.

(f) Exhaust silencer: Reduce the noise generated by the operation of the fan to avoid affecting the health of the experimenters.

(g) Digital pressure display: The display connects to multiple pressure sensors to show pressure data, allowing convenient reading and recording of pressure changes during the experiment.

2.2. Experimental Method

(a) Preliminary Setup: Record the environmental parameters such as ambient temperature and atmospheric pressure before starting the experiment. Calibrate the digital pressure indicator for accurate readings. Check the equipment connections to ensure that the pressure tube is properly connected, and the backwards impeller is properly installed in the casing. During the experiment, keep away from the fan and wear ear defender.

(b) Procedure: Initially, close the sliding valve completely, set the fan to its highest speed and adjust it to 2700 ± 50 rpm after the air speed has stabilized. Then record the pressure data ($\Delta p_1, p_2, p_3$), rotational speed (rpm) and electrical power consumption (W) after the air speed has stabilized again. Then adjust the sliding valve and increase the opening of the sliding valve gradually by 10% each time until it is fully open. Record data after each adjustment until the fan was stabilized. Adjust the fan speed to 2000 ± 50 rpm and 1000 ± 50 rpm, repeat the above steps and record the data accordingly.

(c) Recording measurements: Fill in the table with the measured data and calculate the key parameters.

3. BASIC RESULTS

Table 1. Basic data from Test 1

Slide Valve opening percentages	Δp_1 Pa	p_2 Pa	p_3 Pa	Rotational speed (rpm)	P_{elec} W
0%	0	53	792	2710	80
10%	-54	-45	722	2708	104
20%	-162	-119	678	2706	127
30%	-310	-211	609	2705	148
40%	-488	-323	505	2704	169
50%	-636	-429	398	2703	184
60%	-800	-535	288	2702	195
70%	-912	-620	198	2701	202
80%	-978	-676	133	2701	208
90%	-1020	-715	88	2700	210
100%	-1056	-724	80	2701	210

Table 2. Basic data from Test 2

Slide Valve opening percentages	Δp_1 Pa	p_2 Pa	p_3 Pa	Rotational speed (rpm)	P_{elec} W
0%	6	34	434	2000	38
10%	-54	-45	398	1999	44
20%	-82	-62	373	2000	52
30%	-156	-112	336	2000	61
40%	-254	-175	278	1997	69
50%	-358	-238	214	1995	74
60%	-432	-291	160	1996	82
70%	-496	-338	113	1995	86
80%	-562	-367	74	1996	88
90%	-590	-392	51	1994	88
100%	-594	-394	46	1996	88

Table 3. Basic data from Test 3

Slide Valve opening percentages	Δp_1 Pa	p_2 Pa	p_3 Pa	Rotational speed (rpm)	P_{elec} W
0%	10	13	115	1005	14
10%	2	1	107	1005	15
20%	-12	-12	97	1004	16
30%	-30	-25	89	1003	16
40%	-52	-38	76	1003	17
50%	-74	-58	58	1004	18
60%	-96	-70	45	1005	19
70%	-110	-82	32	1005	19
80%	-122	-90	24	1005	19
90%	-129	-95	18	1005	19
100%	-132	-96	17	1005	19

4. FAN CHARACTERISTICS AT THE THREE FAN SPEEDS

4.1. Results in Tabular

Table 4. Results from Test 1

Q_v m^3/s	Δp_{fan} Pa	Ω rads/s	P_{use} W	P_{elec} W	η_{ov} %
0.0000	739	283.79	0.0000	80	0.0000
0.0417	767	283.58	31.9626	104	30.7332
0.0722	797	283.37	57.5261	127	45.2962
0.0998	820	283.27	81.8737	148	55.3200
0.1253	828	283.16	103.7265	169	61.3766
0.1430	827	283.06	118.2724	184	64.2785
0.1604	823	282.95	132.0062	195	67.6955
0.1713	818	282.85	140.0878	202	69.3504
0.1773	809	282.85	143.4721	208	68.9770
0.1811	803	282.74	145.4337	210	69.2542
0.1843	804	282.85	148.1622	210	70.5534

Table 5. Results from Test 2

Q_v m^3/s	Δp_{fan} Pa	Ω rads/s	P_{use} W	P_{elec} W	η_{ov} %
0.0139	400	209.44	5.5563	38	14.6218
0.0417	443	209.33	18.4608	44	41.9563
0.0514	435	209.44	22.3381	52	42.9578
0.0708	448	209.44	31.7314	61	52.0188
0.0904	453	209.13	40.9416	69	59.3356
0.1073	452	208.92	48.4986	74	65.5387
0.1179	451	209.02	53.1579	82	64.8267
0.1263	451	208.92	56.9596	86	66.2321
0.1344	441	209.02	59.2866	88	67.3711
0.1377	443	208.81	61.0210	88	69.3420
0.1382	440	209.02	60.8129	88	69.1055

Table 6. Results from Test 3

Q_v m^3/s	Δp_{fan} Pa	Ω rads/s	P_{use} W	P_{elec} W	η_{ov} %
0.0179	102	105.2434	1.8292	14	13.0654
0.0080	106	105.2434	0.8501	15	5.6673
0.0196	109	105.1386	2.1412	16	13.3828
0.0311	114	105.0339	3.5409	16	22.1307
0.0409	114	105.0339	4.6618	17	27.4225
0.0488	116	105.1386	5.6588	18	31.4377
0.0556	115	105.2434	6.3897	19	33.6302
0.0595	114	105.2434	6.7803	19	35.6859
0.0626	114	105.2434	7.1406	19	37.5821
0.0644	113	105.2434	7.2782	19	38.3062
0.0652	113	105.2434	7.3623	19	38.7491

4.2. Fan Characteristics in Graphs

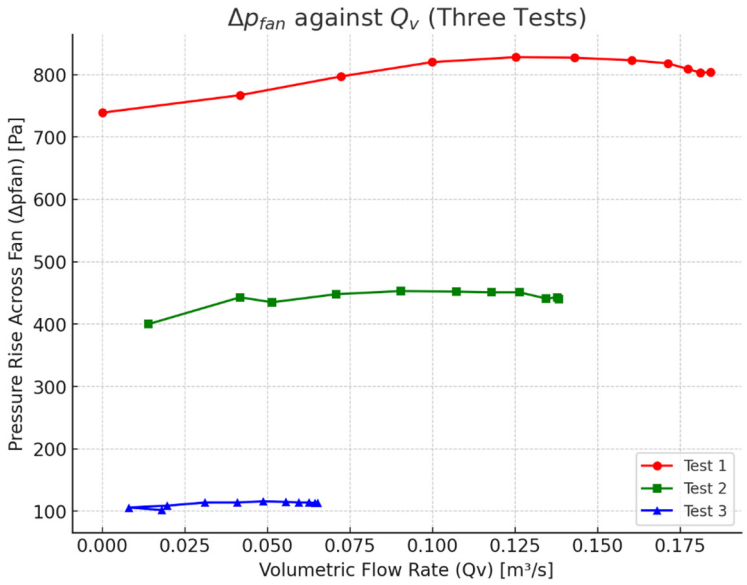

Figure 2. Δp_{fan} against Q_v for the three tests

From the figure, it can be seen that the experimental results are approximately as expected, which means that the characteristic curves of the wind turbine have similar shapes at different rotational speeds, confirming the theory of dynamic similarity. As Q_v increases, the Δp_{fan} of the fan first increases to peak, and then decreases, which is a typical characteristic curve of a centrifugal fan. However, there are some differences in the graph, which may be caused by experimental equipment, environmental factors or operating errors.

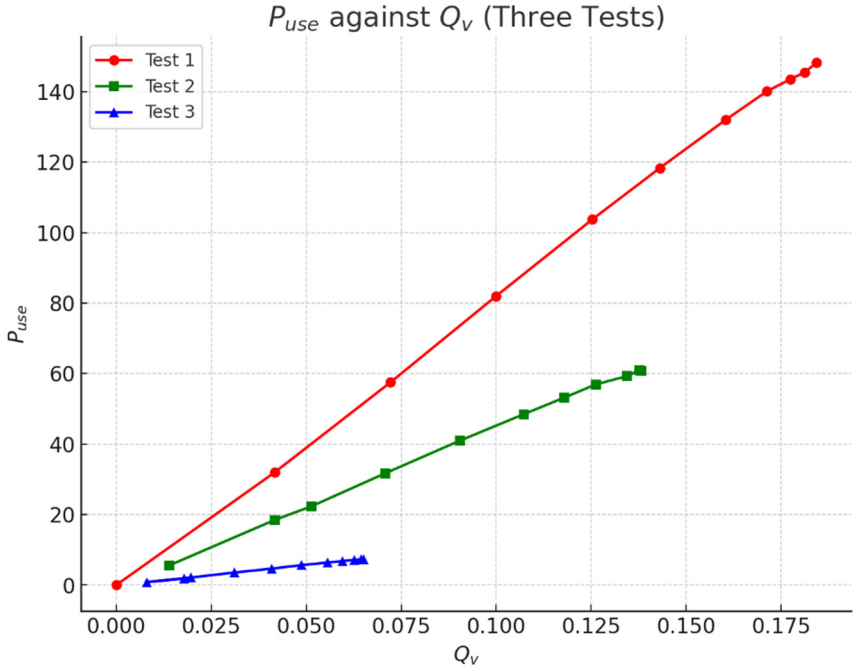

Figure 3. P_{use} against Q_v for the three tests

It can be concluded from the figure that the experimental results are generally agreed with the prediction. P_{use} increases with the increase of Q_v, which demonstrates a near-linear growth trend.

At the same Q_v, the higher the rotational speed, the larger the P_{use}, which is in accordance with the characteristics of the fan [1]. Although the data are basically in accordance with the theory, there are some errors caused by measurement, energy loss, environmental factors.

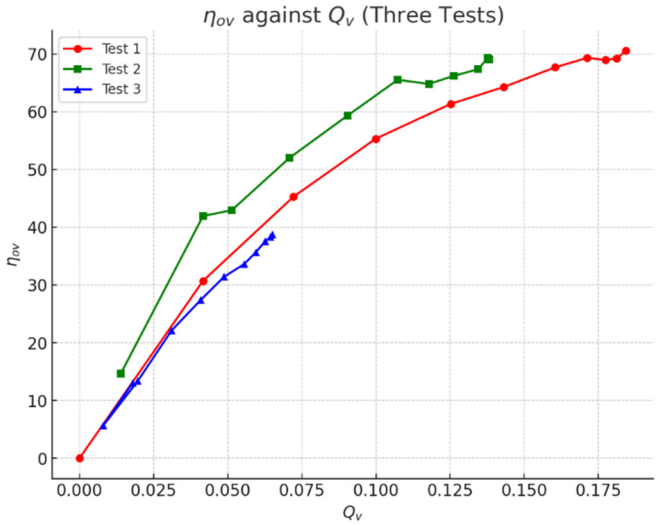

Figure 4. η_{ov} against Q_v for the three tests

As can be seen in Figure 4, the experimental data are generally consistent with the theoretical predictions. The efficiency of the fan ηov rises with the increase of the volume flow rate Qv, and finally tends to stabilize gradually. At medium to high rotational speeds, the fan usually reaches its maximum efficiency at higher flow rates, while at low rotational speeds, the fan has its maximum efficiency at low flow rates. The maximum efficiency of the fan is higher at higher speeds while it is lower at lower speeds, which is consistent with the operating theory of the fan. The trend of the efficiency curves at different speeds is similar, which is in accordance with the characteristics of the fan. There are some errors in the data which may be caused by measurement errors, idealization of experimental assumptions, environmental factors.

5. INVESTIGATION OF DYNAMIC SIMILARITY

5.1. Nondimensional Parameters

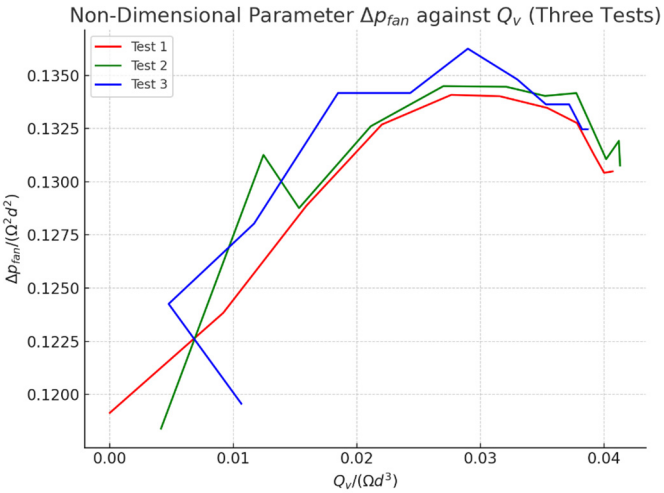

Figure 5. $\frac{\Delta p_{fan}}{\rho \Omega^2 d^2}$ against $\frac{Q_v}{\Omega d^3}$ for the three tests

Figure 5. demonstrates the relationship between the nondimensional parameter $\frac{\Delta p_{fan}}{\rho\Omega^2 d^2}$ and $\frac{Q_v}{\Omega d^3}$. The nondimensional pressure difference increases with increasing flow coefficient and reaches a maximum at 50% or 60% and then begins to decrease. The main trend is in accordance with the fluid theory, which means at lower flow rates, the fan is mainly affected by resistance and the differential pressure rises, while at higher flow rates, the kinetic energy of the fluid dominates and the differential pressure tends to stabilize. From the figure, it can be seen that Test 3 has larger fluctuations in the high flow rate area, which may be due to the experimental instrument error, and environmental factors.

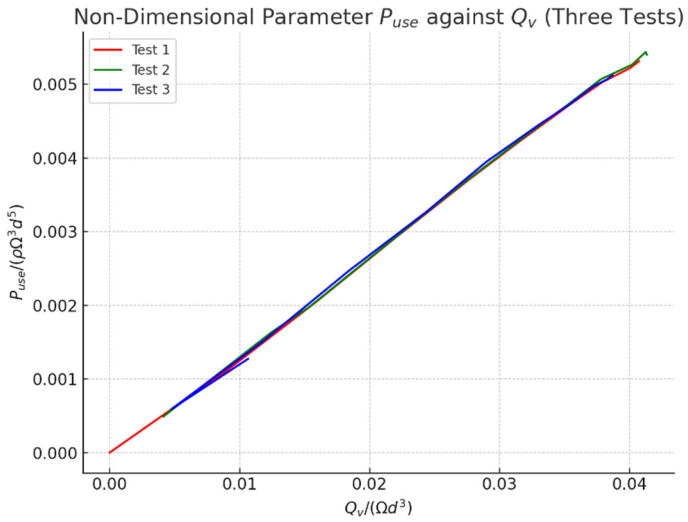

Figure 6. $\frac{P_{use}}{\rho\Omega^3 d^5}$ against $\frac{Q_v}{\Omega d^3}$ for the three tests

As can be seen in Figure 6, the curves of the nondimensional parameters $\frac{P_{use}}{\rho\Omega^3 d^5}$ and flow coefficient $\frac{Q_v}{\Omega d^3}$ show a basically linear increasing trend. It indicates that as the nondimensional flow coefficient increases, the nondimensional power increases accordingly, which is in line with the basic law of fluid dynamics. The curves of the three experiments show a high degree of overlap, indicating small errors.

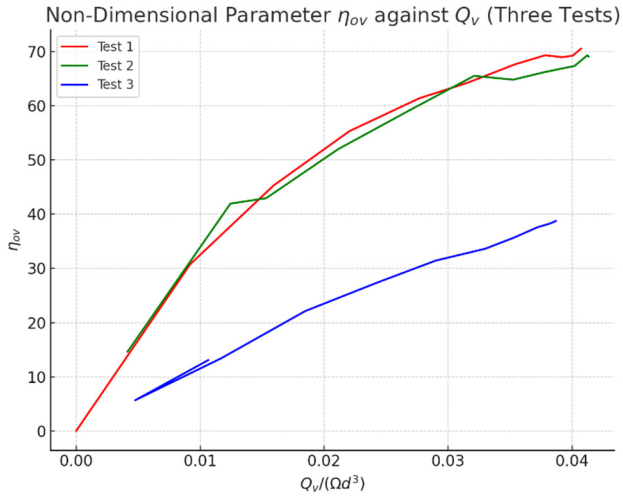

Figure 7. η_{ov} against $\frac{Q_v}{\Omega d^3}$ for the three tests

Figure 7 shows the relationship between the nondimensional parameter overall efficiency η_{ov} and nondimensional flow rate $\frac{Q_v}{\Omega d^3}$. η_{ov} increases rapidly as $\frac{Q_v}{\Omega d^3}$ increases, and then stabilizes, which is typical fan efficiency curve and meets expectations. The data for Test 3 show a large error, which may be caused by experimental equipment errors or environmental factors.

5.2. Example Calculation of Nondimensional Parameters

In the example calculation, in order to show the calculation process more clearly and directly, the data from Test 1 with 10% slide valve opening was used to demonstrate.

First, the density of air needs to be calculated using:

$$\rho = \frac{p_4}{RT_a} = \frac{102700Pa}{287J/kgK\times(273.15+21.9)K} = 1.2128kg/m^3 \quad (1)$$

Where p_4 is the measured atmosphere pressure, *R* denotes the specific gas constant for dry air (*R*=287 J/kgK), T_a is the ambient air temperature.

In this experiment, the nondimensional pressure parameters can be calculated as followed:

$$\frac{\Delta p_{fan}}{\rho\Omega^2 d^2} == \frac{767\ Pa}{1.2128kg/m^3\times(283.58rads/s)^2\times(0.252m)^2} = 0.123837 \quad (2)$$

To describe the characteristics of a pump, the nondimensional power parameter needs to be calculated:

$$\frac{P_{use}}{\rho\Omega^3 d^5} = \frac{31.96W}{1.2128kg/m^3\times(283.58rads/s)^3\times(0.252m)^5} = 0.001137 \quad (3)$$

The nondimensional flow parameter calculation can be calculated as follows:

$$\frac{Q_v}{\Omega d^3} = \frac{0.4167m^3/s}{283.58rads/s\times(0.252m)^3} = 0.009183 \quad (4)$$

5.3. Discussion

(a) Among these three figures, the first one $\frac{\Delta p_{fan}}{\rho\Omega^2 d^2}$ against $\frac{Q_v}{\Omega d^3}$ and second one $\frac{P_{use}}{\rho\Omega^3 d^5}$ against $\frac{Q_v}{\Omega d^3}$ for the three tests display dynamic similarity. For geometrically similar fans, the flow phenomena and physical properties should be similar with the same nondimensional parameters. From Figure 5, it can be seen that the experimental data at different speeds display the dynamic similarity characteristic. The nondimensional pressure increase ($\frac{\Delta p_{fan}}{\rho\Omega^2 d^2}$) follows a similar trend in the three tests. Despite small differences in the low flow rate area, the high degree of similarity between the curves overall indicates the characteristics of dynamic similarity. As seen in Figure 6, the data for the three tests basically overlap in the dimensionless coordinates, displaying dynamic similarity. It indicates that the energy conversion relationship of the fan remains the same in the same dimensionless coordinates.

(b) As can be seen in the third graph, the curve of Test 3 deviates significantly from the data of Test 1 and Test 2 and does not conform to dynamic similarity. The possible reason for this is the increase in mechanical and friction losses at low rotational speeds, which leads to a significant decrease in overall efficiency (η_{ov})and does not correspond to the dynamic similarity of the fluid. It is also possible that at low speeds the airflow over the fan blades may separate, resulting in an increase in vortices, which may in turn reduce the overall efficiency of the fan. Moreover, the slip effect causes the actual fluid exit angle to deviate from the theoretical value. As can be seen in Figure 5, the real characteristic has a significant difference from the result calculated using Euler theory. The slip effect

is more obvious at low speeds, causing the Test3 overall efficiency decrease and breaking the dynamic similarity [3].

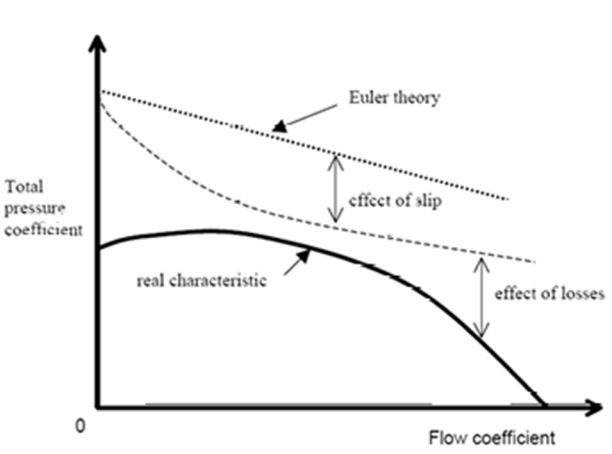

Figure 8. The pressure characteristics of real pumps [2]

(c) From the figures which display dynamic similarity, it can be concluded that high Reynolds numbers have less effect on fan characteristics. The Reynolds number represents the ratio between the kinetic energy of the flow and the fluid friction. A high Reynolds number indicates that inertial forces dominate the flow, which is mainly acted by instability, with less viscous influence. In this experiment, the nondimensional curves of power and pressure at different rotational speeds show an overlapping trend, which indicates that dynamic similarity is maintained under such conditions. It suggests that the fan performance does not change significantly with changes in the Reynolds number if the Reynolds number is high enough. A sample calculation of Test 1, 10% opening is as follows:

$$Re = \frac{\rho \Omega d^2}{\mu} = \frac{1.2128 kg/m^3 \times 283.58 rads/s \times (0.252m)^2}{1.835 \times 10^{-5} kg/ms} = 1190232 \quad (5)$$

Where ρ is the calculated air density (kg/m^3), Ω is the rotational speed ($rads/s$), d is the diameter of the rotor (m), and μ is the dynamic viscosity of the air at room air temperature (kg/ms) [4].

From the sample calculation, it can be seen the Re number is very large. At high Reynolds numbers, the airflow over the fan blades remains turbulent, which reduces the impact of viscous effects on fan performance.

6. CONCLUSION

This experiment analyzed the characteristics of a centrifugal fan with backward inclined blades at different speeds. By measuring the pressure difference, volume flow rate, and efficiency, the performance curves of the fan were plotted. By calculating the nondimensional parameters, the concept of fluid dynamic similarity was verified. The curves of the nondimensional parameters power and pressure difference show the same behavior at different speeds, which confirms the dynamic similarity of the fluid. The experimental results indicated that the performance characteristics of the fan follow dynamic similarity at different rotational speeds, verifying the basic principles of fluid mechanics. However, some errors still exist due to experimental uncertainties, equipment limitations, and environmental factors.

REFERENCES

[1] Khilwani, R., Pandey, K.M., Mahapatra, M.M. (2014). Parametric study of centrifugal fan performance: Experiments and numerical simulation. Available at: https:// www. research gate. net/ publication/267971543_PARAMETRIC_STUDY_OF_CENTRIFUGAL_FAN_PERFORMANCE_EXPERIMENTS_AND_NUMERICAL_SIMULATION [Accessed 7 March 2025].

[2] The University of Nottingham (2025). Lecture 4 Rotodynamic machines PPT [online]. Available at: https:// moodle. nottingham.ac.uk/mod/folder/ view. php? id=7517329 [Accessed 10 March 2025].

[3] Douglas, J.F., Gasiorek, J.M., Swaffield, J.A., Jack, L.B. (2005). Fluid Mechanics. Harlow: Pearson Education. Available at: https://smartbukites.com/wp-content/uploads/2019/04/FLUID-MECHANICS-BY-DOUGLAS00052.pdf [Accessed 10 March 2025].

[4] Engineers Edge. Viscosity of Air, Dynamic and Kinematic. Available at: https://www. engineersedge. com/ physics/ viscosity _of_air_dynamic_and_kinematic_14483.htm [Accessed 12 March 2025].